Phase transitions and Raman spectra of calcite at high pressures and room temperature

Lin-Gun Liu

Research School of Earth Sciences, Australian National University, Canberra, A.C.T., Australia

T. P. Mernagh

Division of Petrology and Geochemistry, Bureau of Mineral Resources, Canberra, A.C.T., Australia

Abstract

High-pressure phase transformations and Raman spectra of calcite at room temperature were studied using single crystals in a diamond-anvil cell under hydrostatic pressure. Calcite displays two reversible phase transformations at high pressures and room temperature. We found, however, that transformation to calcite-II is more likely to occur under nonhydrostatic conditions. This means that it is difficult to locate the transition pressure between calcite-I and calcite-II in a hydrostatic environment. Calcite-III was always found to exist at pressures above 20 kbar at room temperature. It was often observed that calcite-I transformed directly to calcite-III with increasing pressure and that calcite-III always reverted directly to calcite-I with decreasing pressure, without the appearance of calcite-II in either case. The Raman spectra of both calcite-I and calcite-II and the effect of pressure on the spectra of these phases observed in the present study are consistent with those of earlier investigations. However, two distinctive types of Raman spectra of calcite-III are observed, suggesting that the Raman spectrum of calcite-III is itself dependent upon crystallographic orientation.

Introduction

Calcite ($CaCO_3$) is one of the most abundant minerals at the Earth's surface; it is the main constituent of limestone and marble and a small proportion of the shells of many organisms. Calcium carbonate also commonly crystallizes as aragonite, which is 8% denser than calcite at ambient conditions. Although it is generally agreed that aragonite should be the stable high-pressure form of calcite (Jamieson, 1953, 1957), calcite always transforms to metastable calcite-II and calcite-III at higher pressures and at temperatures below about 600 °C (see recent review by Liu and Bassett, 1986). Calcite-II and calcite-III were first discovered by Bridgman (1939), who also delineated the transition boundaries between these phases in the range 25–167 °C.

Raman spectra of calcite-I, calcite-II, and calcite-III have been extensively studied up to 40 kbar at room temperature (Fong and Nicol, 1971; Gillet et al., 1988; Hess and Ghose, 1988). Nonhydrostatic pressure environments were employed in the first two of these investigations. [Although a hydrostatic medium was used, other details of the study by Hess and Ghose (1988) are not known because their work is published in an abstract form only.] We have therefore investigated the Raman spectra of the various forms of calcite using both single-crystal and powder samples in a hydrostatic environment.

Experimental procedure

Clear crystals of Iceland spar, purchased from Ward's Natural Science Company, were used in this work. No chemical analysis of the sample was attempted. A small calcite rhomb (about $30 \times 50 \times 80$ μm) was placed inside the hole (100–200 μm in diameter and 40–80 μm in depth) in a hardened stainless-steel gasket in a standard diamond-anvil cell (e.g., Liu and Bassett, 1986). The natural cleavage plane (101) of the rhomb lay parallel to the surface of the diamond anvil, and thus normal to the laser beam in the Raman studies. A small chip of ruby ($\sim$20 μm) was also placed inside the hole, and an ethanol-methanol (1:4) mixture was used as a pressure medium that yielded hydrostatic pressures up to at least 105 kbar at room temperature. The whole assembly was then sealed by compressing the two diamond anvils. The thickness of the calcite rhombs used in these experiments was chosen to be as close as possible to the thickness of the indented gasket. In this manner, the rhombs were covered with a minimal thin layer of the ethanol-methanol mixture, the Raman spectra of which would otherwise have interfered with those of the various forms of calcite. However, the hydrostatic environment between the sample and anvils was ensured by observing the crush of the sample and checking the reflection at the interface between the upper anvil and fluid. For instance, if a sample was observed to be crusted at 70 kbar with increasing pressure, it is quite certain that the sample was not likely to be subject to a nonhydrostatic environment at pressures below about 60 kbar in the previous experiments. For a given crystal of the sample, the spectra of two or three different spots were often obtained, particularly when different optical domains were observed in the same crystal. However, the Raman spectra never indicated any het-
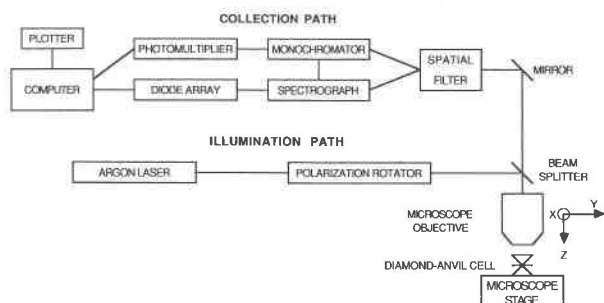
Fig. 1. Schematic diagram of the illumination and collection optics in the Microdil-28 laser Raman microprobe.

erogeneity in a single crystal. In auxiliary experiments, pulverized Iceland spar was loaded instead. For a given experiment, with increasing pressure several spectra were normally recorded, particularly across the transition regions, and a few auxiliary spectra were also obtained with decreasing pressure. Pressures were measured using the ruby-fluorescence technique. The uncertainty in pressure was estimated to be ±2 kbar.

Raman spectra were recorded on a Microdil-28 laser Raman microprobe manufactured by Dilor Co., Lille, France. A schematic diagram of the illumination and collection paths in the Microdil-28 spectrometer are shown in Figure 1. Samples in the diamond-anvil cell are irradiated with a laser beam ~2 μm in diameter at the focus by using an Olympus BH-2 microscope in the reflected-light mode and a 50× ULWD objective, which is also used to bring the sample into focus in white light.

The 514.5-nm green line of a Spectra Physics 2020 3W argon ion laser was used as the excitation source at laser powers of ~600 mW at the source (~60 mW on the sample). The incident laser excitation is linearly polarized in the X direction (see Fig. 1) and travels along a path that includes a half-wave plate for rotating the plane of polarization, the microscope beamsplitter, and the objective. The scattered light is collected at an angle of ~180° by the same objective before passing through the beam splitter and a diaphragm that acts like a spatial filter and controls the effective numerical aperture of the objective without modifying the excitation volume within the sample.

The scattered radiation then passes into an F/5 double monochromator with two plane holographic gratings with 1800 grooves per mm and then to a conventional stigmatic spectrograph with a plane grating and large aperture objectives. Two gratings of 600 and 1800 grooves per mm mounted back to back on a rotating turret provide dispersions of ~1500–2300 cm^{-1} and ~300–400 cm^{-1}, respectively, depending on the absolute wavelength position. In these experiments, Raman spectra were recorded from 75 to 1600 cm^{-1} using a spectral resolution of around 3 cm^{-1} and are accurate to ±1 cm^{-1}.

The Microdil-28 has two detectors and can be operated as a scanning spectrometer by using the monochannel photomultiplier tube located directly after the double monochromator. However, all spectra recorded in this study were obtained by using the multichannel detector situated after the spectrograph. This consists of a multichannel plate intensifier coupled to a 512 photodiode array. Both are cooled to −20 °C by a Peltier semiconductor element. Raman spectra recorded at room temperature were typically acquired after 20 accumulations with 5 s integration time.

The detectors are linked via an IB10 interface to a Cleveland 286 SP personal computer, and the data are recorded and interpreted using software supplied by Dilor. The resulting Raman spectra are then plotted on a Houston Instrument HIPLOT DMP-40 plotter.

PHASE TRANSFORMATIONS

According to Bridgman's compression study, calcite-I transforms to calcite-II near 14 kbar and to calcite-III near 18 kbar at room temperature (see dotted vertical lines in Fig. 2). Merrill and Bassett (1975) stated that these values were revised to 15 and 22 kbar, respectively. However, the Raman spectra of single crystals of these phases obtained in the present study suggest that transition pressures between these phases may differ significantly from those reported above.

Although both calcite-I and calcite-II have been observed to coexist in a single crystal (visually separated by a Becke line) immersed in a hydrostatic pressure medium (Van Valkenburg, 1965), in this study it was found that a single crystal of calcite-I can persist to pressures as high as 19 kbar. It transformed directly to calcite-III when pressure was further increased. Conversely, after calcite-III was formed at high pressures, it always by-passed the field of calcite-II and transformed directly to calcite-I in the pressure range 10–15 kbar when pressure was decreased. In other words, in a hydrostatic environment, single-crystal calcite-I can transform directly to calcite-III with increasing pressure, and calcite-III transforms directly to calcite-I with decreasing pressure, without the appearance of calcite-II in either case. Thus, it appears that the existence of calcite-II in a high-pressure experiment is sensitive to the shear stress in the pressure vessel. On the other hand, we sometimes also observed calcite-II in the pressure range 10–18 kbar in our hydrostatic experiments. These observations are marked in Figure 3. The details of the Raman spectra of these phases are discussed later. Thus, the precise transition pressure, if there is one, between calcite-I and calcite-II at room temperature cannot be satisfactorily located in a hydrostatic pressure environment. This phenomenon may be attributed to the fact that calcite-II is metastable at these P-T conditions and that calcite-II may be formed more easily under nonhydrostatic than under hydrostatic conditions. Fong and Nicol (1971) observed that the transition pressure of calcite-I to calcite-II depended on the orientation
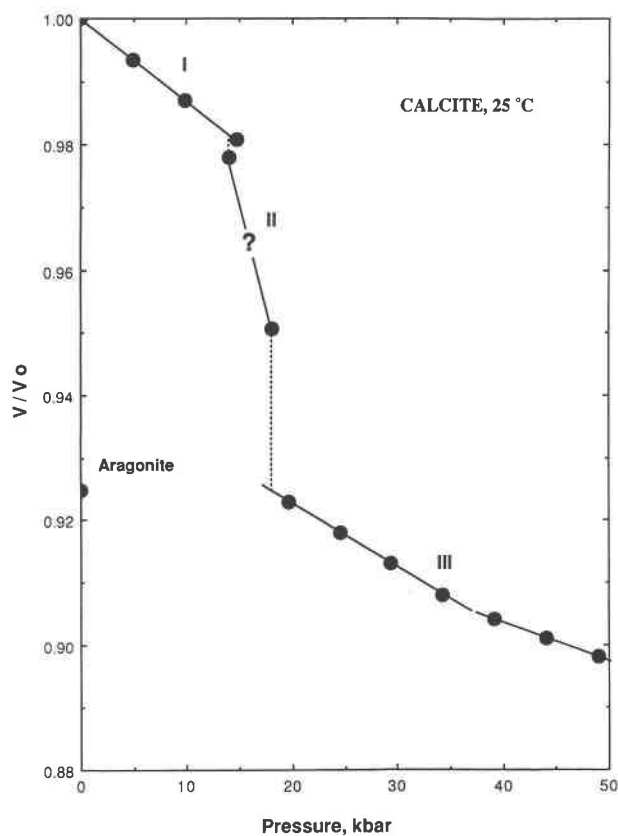
Fig. 2. Compressional data of calcite-I, calcite-II, and calcite-III at room temperature as reported by Bridgman (1939). The line denoted by a question mark represents the compressional behavior of calcite-II inferred from Bridgman's data.
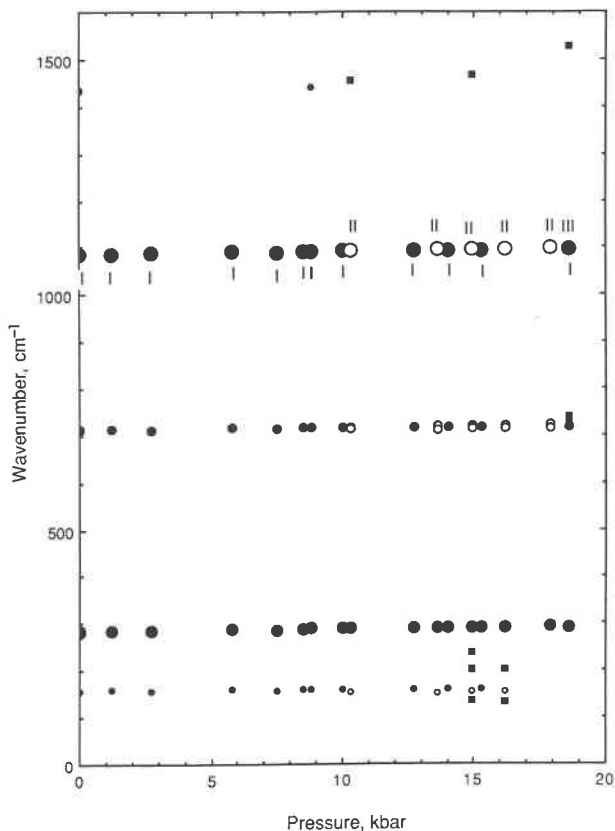

Fig. 3. Pressure dependence of the Raman bands of calcite-I (marked by I), calcite-II (by II) and calcite-III (by III) at room temperature observed in the present study. The size of the circles approximates the relative intensities of these bands. The squares indicate the additional weak bands of calcite-II and calcite-III. The former does not have weak bands near 730 cm^{-1}.

of the sample in their pressure vessel, and often found that calcite-I transformed directly to calcite-III in the parallel position (C parallel to the axis of the high-pressure cell) at pressures as low as 15 kbar.

Except for one experiment at 19 kbar, calcite-III was observed in all experiments carried out at pressures ≥20 kbar in the present study. Thus, the field of calcite-III must extend below 20 kbar at room temperature.

Fong and Nicol (1971) found that no phase transition was observed in aragonite at high pressures and room temperature. As shown in Figure 2, the zero-pressure volume of aragonite is nearly the same as that of calcite-III at 20 kbar. Thus, aragonite would not be expected to transform to calcite-II or calcite-III at high pressures. Quite the contrary, one might expect calcite-III to transform to aragonite at high pressures. Our studies of CaCO$_3$ to over 90 kbar, which is probably the highest pressure to which CaCO$_3$ has ever been subjected, did not imply any such transition however. We have recovered nearly all the samples used in our experiments and have checked their Raman spectra. It was always found that the recovered samples are calcite-I, suggesting that aragonite did not form. Moreover, no reaction has taken place be-

tween the sample and the pressure medium in our experiments.

Single crystals of calcite remain intact across the transition between calcite-I and calcite-II but often break into a few pieces when transforming to calcite-III in a hydrostatic pressure environment. This suggests that the change in volume across the calcite-I ↔ calcite-II transition is rather small, whereas that across the calcite-II (or calcite-I) → calcite-III transition is larger. This is in general agreement with the compressional behavior of calcite (Fig. 2) observed by Bridgman (1939). According to the changes of volume across the calcite-I ↔ calcite-II and calcite-II ↔ calcite-III transitions reported by Bridgman (1939), the line denoted by a question mark in Figure 2 may represent the compressional behavior of calcite-II at room temperature. Figure 2 shows that calcite-II is much more compressible than both calcite-I and calcite-III, which is highly unlikely and is not known of any materials. Thus, Bridgman (1939) may have underestimated the volume discontinuity across the calcite-II → calcite-III transition boundary.
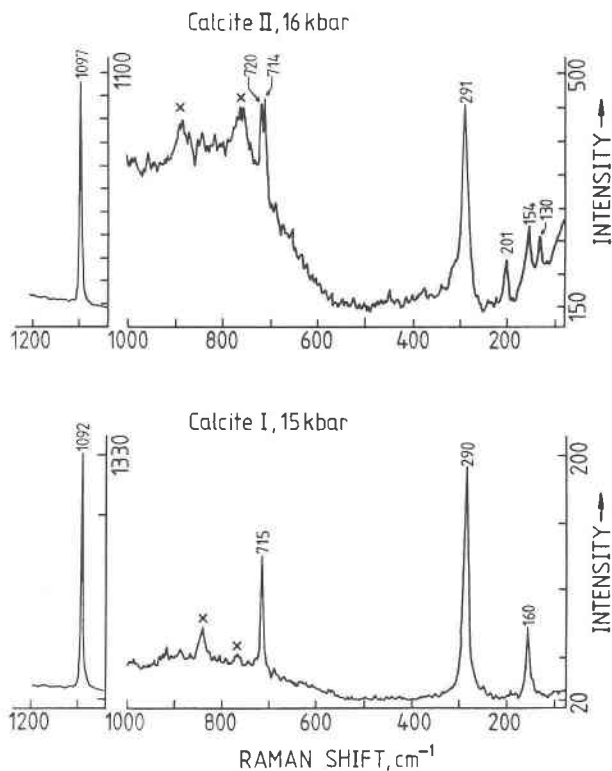
Fig. 4. A direct comparison of the Raman spectrum of calcite-II with that of calcite-I at high pressures. Raman bands from the pressurizing fluid are marked by x.
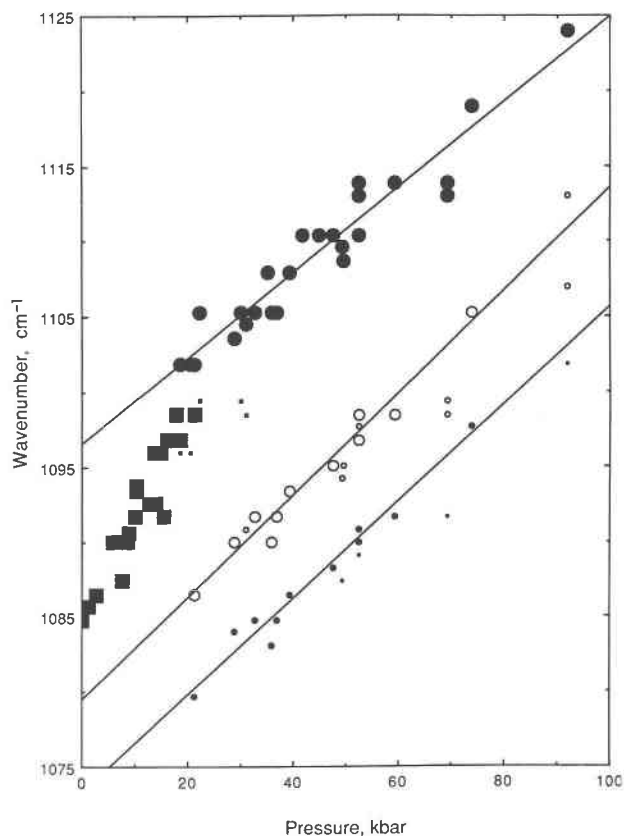

Fig. 5. Pressure dependence of the three strongest Raman bands of calcite-III (denoted by circles) observed between 20 and 100 kbar in the present study. Squares indicate the strongest band of both calcite-I and calcite-II. The size of the symbols indicates the relative intensities of these bands. The straight lines are a least-squares fit for the data for calcite-III. Only the intense lines of the second ($\sim$1085 cm^{-1} at 20 kbar) and the third ($\sim$1079 cm^{-1} at 20 kbar) bands were used in the least-squares fit.

RAMAN SPECTRA

The Raman spectra of calcite-I and calcite-II obtained in this study are identical to those published by Fong and Nicol (1971) and Gillet et al. (1988). There are basically five Raman bands for calcite-I at ambient conditions. The most intense band is the A_{1g} mode at 1085 cm^{-1}. Two sets of doubly degenerate, internal E_g modes are observed at 712 and 1434 cm^{-1}, and the external E_g or lattice modes occur at 282 and 156 cm^{-1}. The external modes are associated with librations of the carbonate ions in the primitive cell around axes normal to the C_3 axis and translations of the CO_3^{2-} ions normal to the C_3 axis, respectively. In addition to a few additional weak bands, the Raman spectrum of calcite-II is in general similar to that of calcite-I. In comparison with the five Raman bands of calcite-I, the bands near 1440 cm^{-1} (at high pressures) for calcite-II split into two (only one can be recognized in the present study owing to the interference of the liquid mixture in the cell), the wavenumber of the most intense band near 1095 cm^{-1} of calcite-II is slightly higher, the bands near 715 cm^{-1} also split into two, and those near 154 cm^{-1} are slightly lower. The bands near 290 cm^{-1} are the second most intense ones and are indistinguishable between calcite-I and calcite-II. These features can easily be seen in the data shown in Figure 3. For a direct com-

parison, the spectrum of calcite-I observed at 15 kbar and that of calcite-II at 16 kbar are shown in Figure 4.

The Raman spectra of calcite-III observed in this study are somewhat different from those reported by Fong and Nicol (1971) and Gillet et al. (1988). Fong and Nicol (1971) observed a very strong Raman band near 1099 cm^{-1} in calcite-III. They observed the intensity of this band to be about one order of magnitude greater than that obtained by both Gillet et al. (1988) and the present study. We also observed that this band was not present at pressures greater than 30 kbar (see Fig. 5). Our results indicate that this band may be caused by residual calcite-II, as suggested by Fong and Nicol. The higher intensity of this band observed in the study by Fong and Nicol would be consistent with the non-hydrostatic pressure conditions of their experiments.

In contrast to previous studies, two distinctive Raman spectra for calcite-III at pressures greater than 20 kbar were observed. One of them is characterized by only one

TABLE 1. Raman spectra of calcite-III observed from two different crystals at 52 kbar and room temperature

Type A	Type B	Type A	Type B
1113 (S)	1110 (S)	209	211 (M)
1098	1097 (S)		193
1089	1090 (M)	183	
866	874	175	
	757		170
749			159
741	741	150	
697	703	143	142
364		137	
356	358		126
	341	115 (M)	115 (M)
316	318 (M)	102 (M)	101 (M)
304			90
	298 (M)		
	275		
264 (M)	261		
254			
236	233 (M)		
228			
	217 (M)		

Note: S stands for strong bands and M for medium bands. All others are weak.
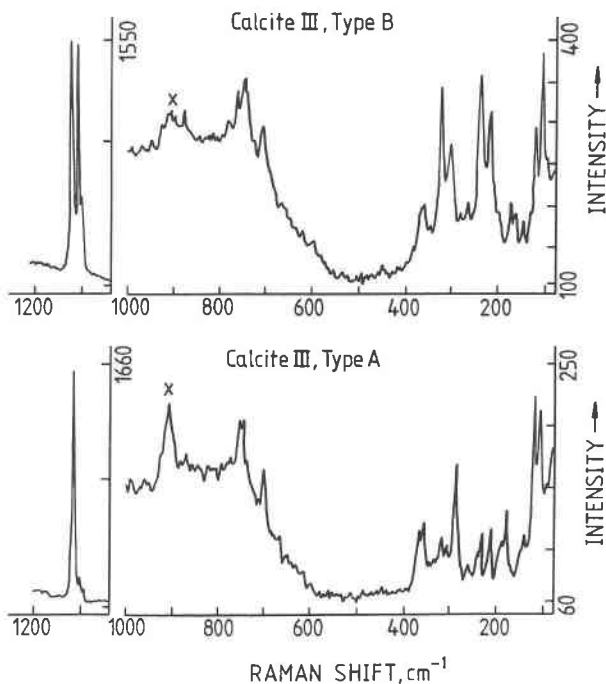

Fig. 6. A direct comparison of the two types of Raman spectra of calcite-III observed in two single crystals in the same cell at 52 kbar. Raman bands from the pressurizing fluid are marked by x.

strong band between 1100 and 1125 cm^{-1} in the pressure range 20–100 kbar (Fig. 6, Type A), in addition to many weak bands at low frequencies. This is basically similar to observations of Fong and Nicol (1971) and Gillet et al. (1988). The second spectrum is characterized by three strong bands. The first of these is the same as that observed earlier, whereas the second band varies from about 1085 to 1105 cm^{-1} in the pressure range 20–75 kbar (it split into two at 92 kbar), and the third one varies from about 1080 to 1098 cm^{-1} in the same pressure range (Figs. 5 and 6). Not only are the intensities of these strong bands different in these two spectra for calcite-III, but the intensities and wavenumbers of many bands at lower frequencies are also rather different. Fortunately, in one experiment at 52 kbar, we observed both types of Raman spectra from two single crystals (which formed when one large crystal broke into several fragments after transition at high pressures) coexisting in the pressure cell. This provided us with an opportunity to compare the two types of Raman spectra of calcite-III under exactly the same conditions. The two types of spectra are shown in Figure 6, and the wavenumbers and the relative intensities of the bands are given in Table 1. Thus, unlike calcite-I, the Raman spectra of which are independent of the orientation (according to Fong and Nicol, 1971), the Raman spectra of calcite-III appear to be strongly dependent upon crystallographic orientation. However, these observations are further complicated by changing the polarization of the laser beam. In one experiment, we recorded two identical spectra of the sample at the same spot using polarizations differing by 90 degrees in the x-y plane of the laser beam. As shown in Figure 5, we observed more of the second type of spectrum (B in Fig. 6 and Table 1) than of the first type (A in Fig. 6 and Table 1) in our studies in the pressure range 20–100 kbar using single

crystals under a hydrostatic environment. Of course, many of the spectra are probably a combination of the two types. The Type A spectrum of calcite-III shown in Figure 6 may itself be a combination of the two types, but with the first type predominating. This is implied by the observation that the Raman spectra for calcite-III were characterized by only one strong band plus weak bands in lower frequencies in many other experiments. Our studies of a polycrystalline sample in a hydrostatic medium revealed a Raman spectrum of calcite-III that is similar to those observed by Fong and Nicol (1971) and Gillet et al. (1988).

No definite assignment has been given to the structure of calcite-III, but X-ray diffraction studies (Davis, 1964) have shown that the c axis has been considerably shortened in comparison with calcite-I and calcite-II. This compression of the c axis has the effect of displacing the carbonate ions from the planes midway between the layers of Ca ions.

Davis (1964) has suggested that the X-ray diffraction pattern of calcite-III may be similar to that of KNO_3-IV with ten molecules per unit cell. According to Jamieson (1956), KNO_3-IV may be isostructural with an ambient $RbNO_3$ structure. Pauling and Sherman (1932) have tentatively assigned this structure to space group C_{3v}^2 with 18 molecules per unit cell. This space group gives $3A_1 + 3E$ vibration modes, all of which are Raman active.

More than 20 Raman lines are observed in both of our calcite-III spectra, as shown in Table 1. This large num-

TABLE 2. Raman frequencies, rate of change and Grüneisen parameters for calcite at ambient conditions and for the strongest bands of calcite-III at 20 kbar and room temperature

ν_i, cm^{-1}	$d\nu_i/d\rho$, cm$^{-1}\cdot$kbar^{-1}	$\gamma_i = I_{in}\nu_i/I_{in}V$
	calcite-I	
1434	0.90	0.47 ± 0.03
1085	0.587	0.41 ± 0.01
713	0.222	0.24 ± 0.01
283	0.527	1.38 ± 0.08
156	0.247	1.18 ± 0.06
	calcite-III	
1102	0.284	0.23 (0.37)*
1086	0.341	0.28 (0.45)
1080	0.323	0.26 (0.43)

* Corresponding to two sets of compressional data for calcite-III (see text).

ber of lines suggests a more complex structure than that indicated above and at least several formula units per unit cell. However, as the X-ray data indicate the structure has similarities with space groups isogonal with point group C_{3v}, those space groups may serve as a basis for the assignment of the Raman spectra. The three strong internal modes observed between 1080 and 1150 cm^{-1} in the spectrum of calcite-III, Type B, correspond with the three predicted A_1 modes. These are all polarized modes and hence are dependent upon the crystal orientation and the polarization of the laser beam. These modes may be expected to be most intense when propagation of the laser beam coincides with the C_3 axis of the carbonate ions. The large decrease in intensity exhibited by two of these modes in the spectrum of calcite-III, Type A, suggests that the laser beam is not aligned with their C_3 axes. In this case, correct laser alignment would also be less likely to occur in polycrystalline samples and may explain why only the Type A spectrum has been previously observed from powder samples.

The other internal modes observed in our calcite-III spectra may be related to the ν_2 and ν_3 modes of the carbonate ion and would be expected to have E-type symmetry by analogy with the spectrum for calcite-I. The large number of external modes are difficult to interpret but may be expected to be mostly E type by analogy with calcite-I. However, some bands show large changes in intensity with different crystal orientations, which suggests that they are also polarized.

The Raman frequencies, the rate of change and the mode-Grüneisen parameters, γ_i, of calcite measured in the pressure range 0–18 kbar and of calcite-III in the pressure range 20–90 kbar are listed in Table 2. The compressional data shown in Figure 2 were used in the calculation of Grüneisen parameters. The rate of increase of the various bands of calcite with pressure (shown in Table 1) are consistent with the average rate of change of these

bands (0.3 to 1.2 cm$^{-1}\cdot$kbar^{-1} in the range 0–10 kbar) reported by Fong and Nicol (1971), and with those (0.5 to 1.0 cm$^{-1}\cdot$kbar^{-1} in the range 0–5 kbar) reported by Gillet et al. (1988). Both the change of the frequencies and the compressional data of calcite-II are poorly known; therefore, it is not very useful to list these properties for calcite-II in Table 2. As discussed by Bridgman (1939), compressional data for calcite-III are somewhat peculiar. Data between 20 and 35 kbar can be fitted with a linear regression, and those above 35 kbar with another linear regression. Thus, based on these two lines, we have listed two sets of the Grüneisen parameters for calcite-III. Only the strongest three bands for calcite-III were listed in Table 2, because so many weak bands were observed at lower frequencies and because the patterns of these weak bands are rather different from experiment to experiment (e.g., Fig. 6). Thus, the recognition of these weak bands at various pressures become very difficult, and the data obtained cannot be accepted without ambiguity.

ACKNOWLEDGMENTS

REFERENCES CITED

Bridgman, P.W. (1939) The high-pressure behavior of miscellaneous minerals. American Journal of Science, 37, 7–18.

Davis, B.L. (1964) X-ray diffraction data on two high-pressure phases of calcium carbonate. Science, 145, 489–491.

Fong, M.Y., and Nicol, M. (1971) Raman spectrum of calcium carbonate at high pressures. Journal of Chemical Physics, 54, 579–585.

Gillet, P., Malezieux, J.-M., and Dhamelincourt, M.-C. (1988) Microraman multichannel spectroscopy up to 2.5 GPa using a sapphire-anvil cell: Experimental set-up and some applications. Bulletin de Minéralogie, 111, 1–15.

Hess, N.J., and Ghose, S. (1988) Raman spectra of the calcite-CaCO$_3$(II) structural phase transition as a function of pressure (abs.). EOS, 69, 500.

Jamieson, J.C. (1953) Phase equilibrium in the system calcite-aragonite. Journal of Chemical Physics, 21, 1385–1390.

——— (1956) Some X-ray diffraction data on KNO$_3$IV, a high pressure phase. Zeitschrift für Kristallographie, 107, 65–71.

——— (1957) Introductory studies of high-pressure polymorphism to 24,000 bars by X-ray diffraction with some comments on calcite-II. Journal of Geology, 65, 334–343.

Liu, L., and Bassett, W.A. (1986) Elements, oxides and silicates: High-pressure phases with implications for the Earth's interior, 250 p. Oxford University Press, New York.

Merrill, L., and Bassett, W.A. (1975) The crystal structure of CaCO$_3$(II), a high-pressure metastable phase of calcium carbonate. Acta Crystallographica, B31, 343–349.

Pauling, L., and Sherman, J. (1932) Note on the crystal structure of rubidium nitrate. Zeitschrift für Kristallographie, 84, 213–216.

Van Valkenburg, A. (1965) Conference Internationale sur-les-Hautes Pressions, Le Creusot, Saone-et-Loire, France, 2–6 August (not seen; extracted from Acta Crystallographica, B31, 343, 1975).